

THE TRANSPORT OF PHOTOCHEMICAL POLLUTANTS TO THE BACKGROUND TROPOSPHERE

CATHERINE C. BAZZELL and LEONARD K. PETERS

Department of Chemical Engineering, University of Kentucky, Lexington, KY 40506, U.S.A.

(First received 21 July 1980 and in form 1 October 1980)

Abstract—A photochemical model incorporating plume dilution effects was used to estimate the fractions of NO_x and hydrocarbons remaining in an urban plume after travel distances on the order of 80–330 km from the urban area. The model considered variable input parameters such as initial concentrations, time of day of plume emergence from the urban area, and atmospheric stability, but did not consider deposition. Approximately 15–20% of the NO_x and 25–30% of the olefins that were initially present at 11:00 am remained in the plume at 10:00 pm. Predicted NO_x transformation rates of 5–20% h^{-1} were in good agreement with recent measurements for urban plumes from Boston and Phoenix. The calculations also showed that plumes dispersing over long distances exhibited diurnal variations of NO_x typical of the urban atmosphere. However, the magnitude of the secondary NO_x peak was negligible in comparison to the primary peak, suggesting that very small amounts of NO_x are transferred to the background in chemical forms that can produce additional NO and NO_2 by photolytic processes on the second day. Larger HC/NO_x ratios led to much higher downwind O_3 levels and thus lower NO_x and olefin concentrations. Changes in atmospheric stability substantially altered the species concentration profiles, but compensating factors resulted in insignificant differences in the fractions of the species remaining for different atmospheric stability conditions.

1. INTRODUCTION

Background air has been variously defined as that which is as clean as one would have expected to find prior to the advent of technological civilization, the least modified air that presently exists globally, or that air which is adjacent to but outside of a given area, e.g. rural vs urban (Stampfer and Anderson, 1975). Many studies have been undertaken to determine concentration levels of photochemical pollutants in clean air and have shown wide ranges of background levels for NO , NO_2 and O_3 in part due to varying effects from anthropogenic sources.

The objective of the present work was to study the phenomena occurring as a chemically reacting plume, with specific initial concentrations of NO , NO_2 , O_3 and hydrocarbons, emerges from an urban area and is advected to the background troposphere. By determining the fractions of NO_x and hydrocarbons that are transported to distances far enough to be considered background, a better understanding of the global NO_x and hydrocarbon budgets can be realized.

A 56-step, lumped kinetic mechanism for photochemical smog, which includes current information on pertinent chemical reactions and rate constants for these reactions developed by Falls and Seinfeld (1978), and Falls *et al.* (1979), was used in these studies. (Their process accounting for wall losses of O_3 was not included in the present analysis.) The organic species present in the mechanism are divided into six lumped classes: (1) ethylene; (2) higher molecular weight olefins; (3) paraffins; (4) formaldehyde; (5) higher molecular weight aldehydes and (6) aromatics. Fifteen

time-dependent differential equations and eleven algebraic equations which describe the mechanism were solved simultaneously using the integration technique proposed by Fowler and Warton (1967), which is particularly useful for ordinary differential equations with widely separated eigenvalues.

Since a plume emerging from an urban area is also being diluted while the chemical reactions are occurring, the kinetic equations were modified to simulate both phenomena. This procedure thus includes in a simple fashion, the simultaneous effects of both processes as the species concentrations are changing.

2. EVALUATION OF THE MODEL

Many of the atmospheric chemistry models available today, including the Seinfeld–Falls (S–F) mechanism, have been compared with data from smog chamber experiments rather than actual measurements of atmospheric concentrations. In the present study, the S–F model was initially tested against data from the Los Angeles Reactive Pollutant Program (LARPP), which was established to measure chemical reactions occurring in specific parcels of air and to provide useful data for testing models of photochemical smog formation.

2.1. Representation of the photolytic rate constants

Since the photochemical mechanism was being used for a diurnally varying solar flux, the photolysis reactions had to reflect this. These were expressed empirically as a function of solar zenith angle. Five of the eight rate constants were reported by Kitada

(1979). These rate constants were calculated from solar flux and quantum yield considerations as

$$k = \sum_{\lambda} a(\lambda) F(\lambda, \theta, z) q(\lambda), \quad (1)$$

or

$$k = \sum_{\lambda} k_a(\lambda) q(\lambda), \quad (2)$$

where $k_a(\lambda) = 2.303 \varepsilon(\lambda) F(\lambda, \theta, z)$; $a(\lambda)$ is the absorption cross section ($\text{cm}^2 \text{molecule}^{-1}$); $F(\lambda, \theta, z)$ is the actinic flux ($\text{photons cm}^{-2} \text{s}^{-1}$); $q(\lambda)$ is the quantum yield; $\varepsilon(\lambda)$ is the absorption coefficient ($\text{cm}^2 \text{molecule}^{-1}$); and k_a is the absorption rate (s^{-1}). The independent variables λ , z , and θ represent the wavelength of the incident energy, the altitude, and solar zenith angle, respectively. Good empirical relations were obtained to describe the photolysis of NO_2 , O_3 forming $\text{O}({}^1\text{D})$, HCHO and HONO .

The rate constant for the reaction $\text{O}_3 + h\nu \rightarrow \text{O}_2 + \text{O}({}^3\text{P})$ was reported by Hampson and Garvin (1977) as $2.034 \times 10^{-2} \text{ min}^{-1}$ at a solar zenith angle of approx. 35° . Using the general form $k = C_1 \exp(C_2/\cos \theta)$ and assuming C_2 remains the same for all O_3 photolysis reactions, C_1 was calculated.

Recent results reported by Taylor *et al.* (1980) indicate that the photo dissociation rate of CH_3ONO at a solar zenith angle of 45° is about twice that for HONO . However, results for other alkyl nitrites are apparently not available. The photolysis of CH_3CHO is lower than that of HCHO , probably by a factor of two to three at noon time based on the studies of Weaver *et al.* (1976). Again, results for other aliphatic aldehydes are quite limited. Thus, for the present study, the rate constants for the photolysis of RCHO and RONO type compounds were taken to be the same as for the photolysis of HCHO and HONO , respectively. Assuming conditions at or near ground level, rate constants for all eight photolytic reactions were calculated and are shown in Table 1.

2.2. Comparison with LARPP data

Calvert (1976a) reported data obtained from Operation No. 33, which was a selected single day of the LARPP, 5 November 1973. The data were shown as concentration-time plots for NO , NO_2 and O_3 for various elevations. Calvert (1976b) also reported

Table 1. Photolytic rate constants for the model

Reaction	Rate constants (ppm-min units)
$\text{NO}_2 + h\nu \rightarrow \text{NO} + \text{O}({}^3\text{P})$	$0.93 \exp(-0.48/\cos \theta)$
$\text{O}_3 + h\nu \rightarrow \text{O}_2 + \text{O}({}^1\text{D})$	$1.135 \times 10^{-2} \exp(-1.930/\cos \theta)$
$\text{HONO} + h\nu \rightarrow \text{OH} + \text{NO}$	$0.165 \cos \theta$
$\text{HCHO} + h\nu \rightarrow \text{HO}_2 + \text{HCO}$	$2.353 \times 10^{-3} \exp(-0.825/\cos \theta)$
$\text{HCHO} + h\nu \rightarrow \text{H}_2 + \text{CO}$	$7.35 \times 10^{-3} \exp(-0.652 \cos \theta)$
$\text{O}_3 + h\nu \rightarrow \text{O}_2 + \text{O}({}^3\text{P})$	$0.215 \exp(-1.930/\cos \theta)$
$\text{RCHO} + h\nu \rightarrow \text{RO}_2 + \text{HCO}$	$2.353 \times 10^{-3} \exp(-0.825/\cos \theta)$
$\text{RONO} + h\nu \rightarrow \text{RO} + \text{NO}$	$0.165 \cos \theta$

alkane, olefin and aromatic concentrations obtained at 8:23 am at an elevation of 425 ft. Figure 1 shows the comparison of the model results with the LARPP data. The solar declination angle and latitude were set to correspond to Los Angeles on the date the data were reported. These results compare quite satisfactorily, as shown by similar maximum concentration values and corresponding trends. Any inconsistencies could be due to factors not included in the model, such as traffic flow and local industrial areas. Based on these favorable comparisons, it was concluded that the model adequately simulated real atmospheric behavior.

3. DILUTION OF THE URBAN PLUME

A dilution parameter was used to represent the phenomena occurring as the urban plume disperses in the atmosphere and as the individual chemical species in the plume are diluted. Consider a mass balance for each chemical species in the mechanism, letting $f_i(k_1, k_2, \dots, k_n, c_1, c_2, \dots, c_m)$ represent the chemical kinetics of species i . The plume behaves as a reactor of continuously increasing volume, V , and it is assumed that entrainment of background air and surface deposition do not substantially affect the mass of species in the plume. Depending on the species, these two phenomena can partially offset one another since the former adds mass and the latter depletes mass. The significance of entrainment is greater for species with higher background concentrations, two such species being CH_4 and O_3 . Entrainment of CH_4 would be relatively unimportant due to its low reactivity, while O_3 entrainment would only become important at large downwind distances from the urban edge where the background level is approached. At such distances, it will be seen that the entrainment factor due to plume spreading becomes quite small. Surface deposition has not been included due to the lack of adequate data describing this process for most of the photochemical pollutants. In any event, surface losses would further decrease the NO_x remaining in the plume, and the present analysis should provide conservative estimates. Thus, under these conditions

$$\frac{d(Vc_i)}{dt} = Vf_i(k_1, k_2, \dots, k_n, c_1, c_2, \dots, c_m). \quad (3)$$

Differentiating the left-hand side of Equation (3) and rearranging yields

$$\frac{dc_i}{dt} = f_i(k_1, k_2, \dots, k_n, c_1, c_2, \dots, c_m) - c_i \frac{d\ln V}{dt}. \quad (4)$$

The second term on the right-hand side represents the spreading of the plume which can be added to the kinetic rate expressions represented by the functions f_i .

A usable form of the dilution was required to supplement the Seinfeld-Falls chemistry and is schematically represented in Fig. 2. Region a represents the source of the plume to be studied which is a hypothetical urban area of length, x_0 , and urban plume

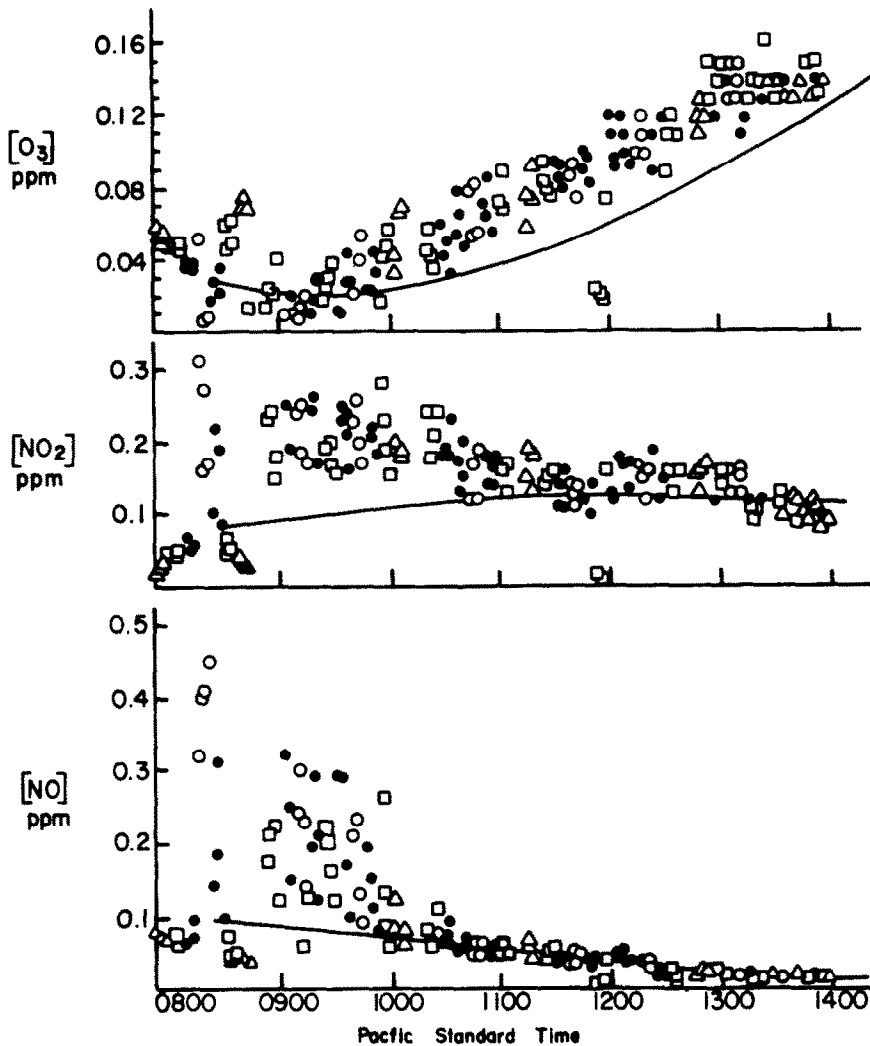


Fig. 1. Comparison of simulation results with the real plume data of LARPP Operation No. 33. Symbols designate different elevation regions: triangles, 768–838 ft; squares, 600–664 ft; darkened circles, 420–437 ft; and open circles 218–230 ft. Solid line represents simulation results.

cross-sectional area, A_0 . Point b represents the plume at any time, t , and distance, x , from the edge of the urban area. Neglecting dispersion of the plume in the direction of advection, the cross-section of the plume at any time can be related to the standard deviations of

the dispersion. Thus, if K is a proportionality constant the area is $K\sigma_x\sigma_z$, where σ_x and σ_z are the horizontal and vertical standard deviations from the centerline of the plume. The Gifford-Pasquill atmospheric stability categories can be used to estimate these standard

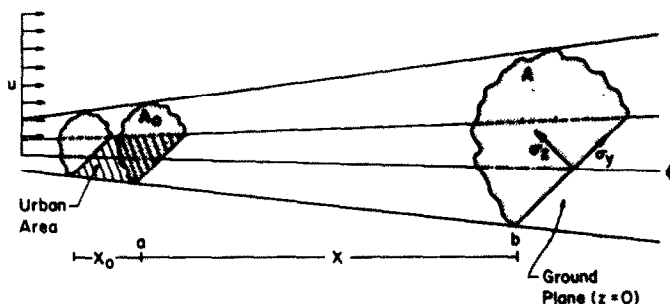


Fig. 2. Schematic representation of plume dilution.

deviations as functions of downwind distance (Gifford, 1961; Pasquill, 1962).

By changing from a Lagrangian to an Eulerian coordinate system and letting δx be a small length of the plume in the axial direction

$$\frac{d(\ln V)}{dt} = U \frac{d(\ln V)}{dx} = U \frac{d(\ln \delta x A)}{dx}, \quad (5)$$

where U is the wind speed. For negligible axial dispersion, δx is constant, and recognizing that $A = K\sigma_y\sigma_z$,

$$U \frac{d(\ln K\sigma_y\sigma_z)}{dx} = U \left[\frac{d(\ln \sigma_y)}{dx} + \frac{d(\ln \sigma_z)}{dx} \right] \quad (6)$$

The equations defining σ_y and σ_z as functions of downwind distance, $x + x_0$, are then written as follows

$$\sigma_y = \alpha_y(x + x_0)^{m_y}, \quad (7)$$

$$\sigma_z = \alpha_z(x + x_0)^{m_z}. \quad (8)$$

Thus, Equation (6) becomes

$$U \left[\frac{d(\ln \sigma_y)}{dx} + \frac{d(\ln \sigma_z)}{dx} \right] = U \left(\frac{m_y + m_z}{x + x_0} \right), \quad (9)$$

and transforming back to a Lagrangian system

$$\frac{d(\ln V)}{dt} = \frac{m_y + m_z}{t + x_0/U}. \quad (10)$$

The variables m_y and m_z were determined by approximating the Gifford-Pasquill curves as straight lines on logarithmic coordinates and calculating the slopes. Values for m_y and m_z were determined for the various Gifford-Pasquill stability categories.

4. RESULTS AND DISCUSSION

In order to study the transformation and removal of NO_x and hydrocarbons (HC), the simulated urban plume was advected from the edge of the urban area at different times of the day. Simulations with conditions varying the atmospheric stability and initial HC/NO_x ratio were also made to study what changes might be anticipated. Finally, NO_x transformation/removal rates for the transported plume at various HC/NO_x ratios were also calculated. The results presented correspond to a solar declination angle of 0° (first day of spring or fall) and a latitude of 35° .

4.1. Concentration profiles for a dispersed urban plume

Numerical data were obtained for plumes leaving the urban area at 8:30 am, 11:00 am, 2:00 pm and 4:00 pm. All of the simulations showed decreasing NO , NO_2 and hydrocarbon concentrations with elapsed time. A late afternoon O_3 peak was seen for all cases except the 4:00 pm plume where the sunlight intensity had decreased to the point that significant O_3 was no longer being produced. Figure 3 shows the concen-

tration profiles for NO , NO_2 , O_3 and hydrocarbons for plume emergence times of 8:30 am and 4:00 pm.

The NO_x decrease was significantly affected by the chemistry as shown by Fig. 4. This plot shows the fraction of NO_x remaining in the plume at various times of the day for the four plume emergence times. It should be noted that this fraction would remain unity if there were no chemical reactions or other removal processes occurring. The fraction decreased slowly in the morning hours but became more rapid later in the day. The fraction of NO_x had dropped to less than 20% of that originally present by 10:00 pm. The rapid decrease noted with the 4:00 pm plume is most probably due to relatively high free radical concentrations (e.g. OH and RO_2) and the absence of significant photolysis rates. Thus, the formation of nitrates and nitrates was strongly favored.

Since olefins form the most reactive hydrocarbon class, the fraction of olefin remaining in the plume was examined over a significant time period for three different initial HC/NO_x ratios (see Fig. 5). It can be seen that the smallest HC/NO_x ratio led to higher relative olefin concentrations remaining which, like the NO_x level, was apparently due to the formation of lower free radical concentrations and thus smaller amounts of olefin destruction by reaction with OH. By 10:00 pm, the fraction of olefin remaining in the plume had dropped to approx. 25% for the middle HC/NO_x ratio and to only about 12% for the doubled HC/NO_x ratio.

4.2. Concentration variations at specific downwind distances

Figure 6 shows the concentrations of NO , O_3 and NO_2 that would be observed at specific distances downwind from an urban area during a given time period. Figure 6(a) shows that the NO concentration at a given time was smaller at further downwind distances. As sunset was approached, these variations in NO concentrations became less since chemistry was less important. Regardless of the distance downwind, the NO concentration was negligible at sunset due to consumption by the excess O_3 that was present in the plume.

Figure 6(b) shows the results for O_3 . Rubino *et al.* (1976) have shown similar behavior for an actual plume from New York City. They suggested that the late afternoon O_3 peaks in Connecticut, which occurred several hours after maximum sunlight intensity, were caused by O_3 and O_3 -precursors (HC and NO_x) that were generated in New York City and drifted into Connecticut on the afternoon sea breeze. The simulated results of this model, which predicted sufficient NO , NO_2 , and hydrocarbon concentrations downwind so that O_3 production could occur, support that theory.

An unexpected phenomenon is shown in Fig. 6(c). In the later afternoon, higher concentrations of NO_2 were predicted further downwind. This could be due to the presence of excess O_3 levels and negligible NO . In

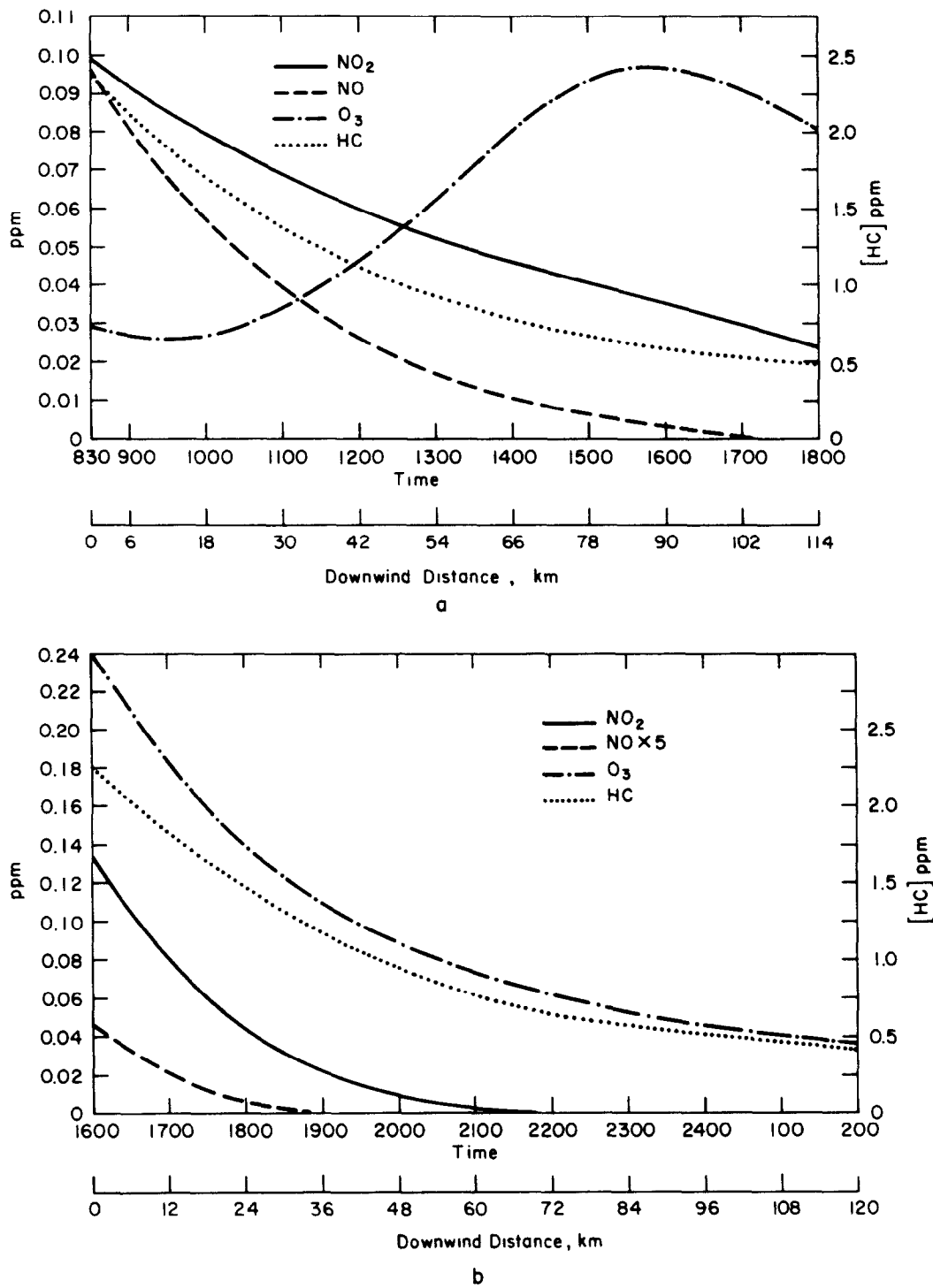


Fig. 3. Concentrations of NO, NO₂, HC and O₃ as a function of distance or travel time from the urban area:
(a) plume emergence time of 8:30 am and (b) plume emergence time of 4:00 pm.

the evening, NO₂ was not being formed by NO oxidation but was simply being diluted.

4.3. Comparisons with background data

There have been numerous studies to determine the background, or clean air, concentrations of NO, NO₂

and O₃. Breeding *et al.* (1973) reported background concentrations for NO₂ in the range of 1–3 ppb, based on daily averaged data measured at 89–121 km from St Louis. Non-urban values at Piedmont, North Carolina have been reported by Ripperton *et al.* (1970) for NO₂ and NO as 5.6 ppb and 1.9 ppb, respectively.

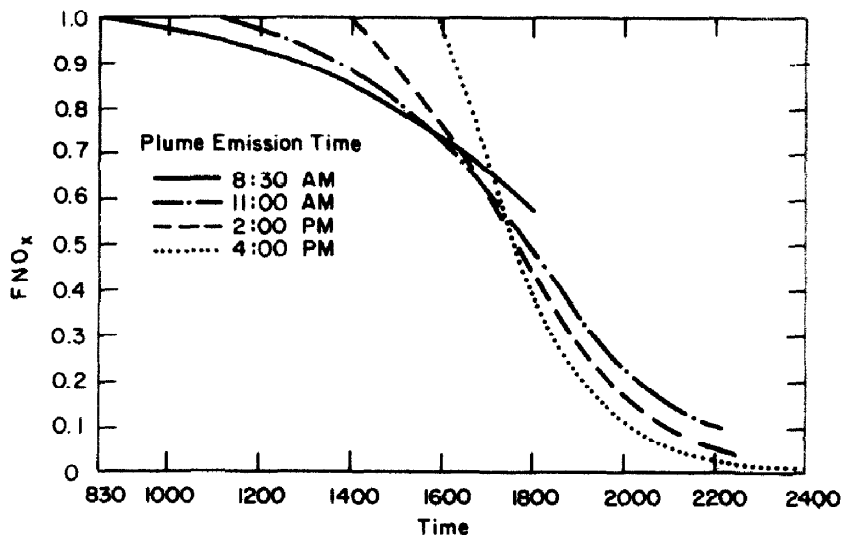


Fig. 4. Fraction of NO_x remaining in the urban plume vs. travel time.

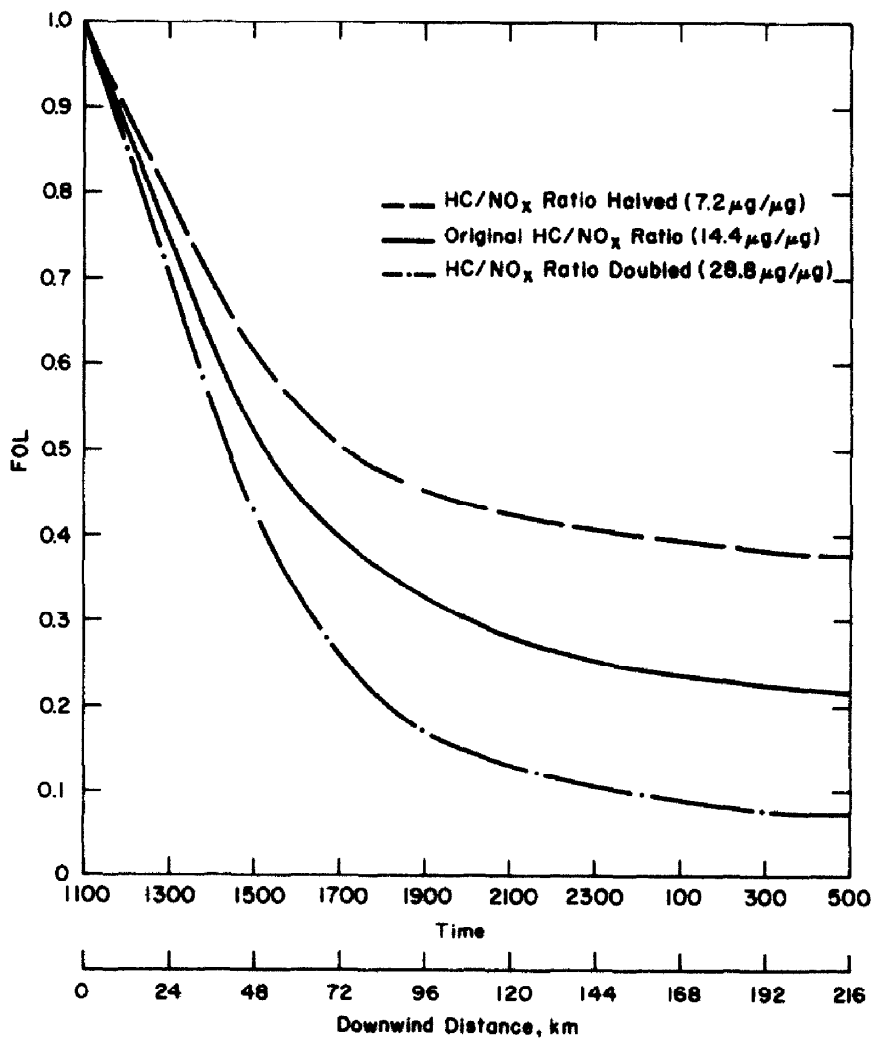


Fig. 5. Fraction of olefin remaining in the urban plume vs. distance or travel time from the urban area. A greater fraction of olefin is removed from the plume at higher HC/NO_x ratios.

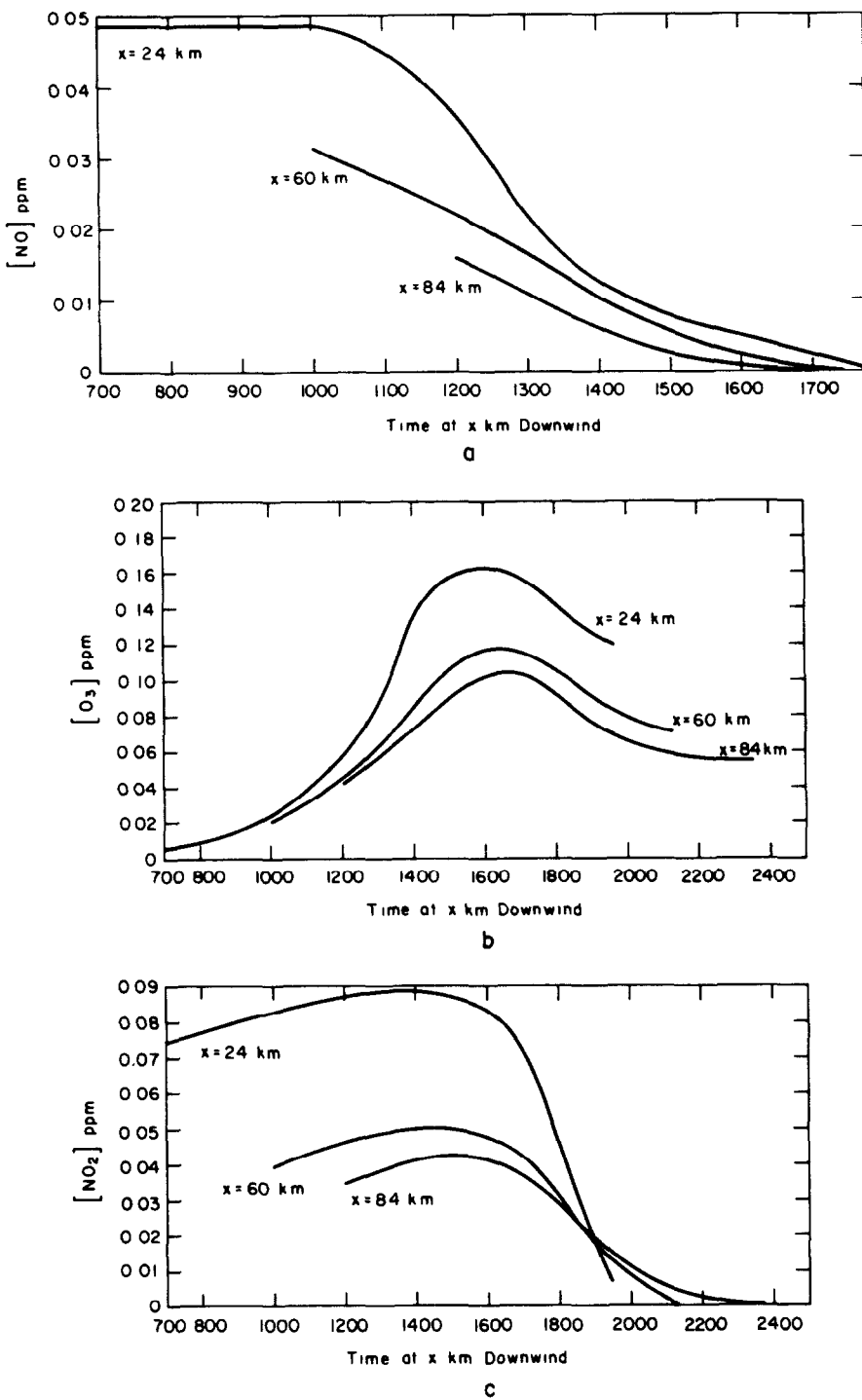


Fig. 6. Concentration of species as a function of time observed at 24, 60 and 84 km from the urban area: (a) NO; (b) O₃ and (c) NO₂.

Mean monthly O₃ concentrations ranging from 20 ppb in January 1975 to 39 ppb in July 1975 have been reported by Mohnen and Hogan (1977) for the rural Whiteface Mountain area in New York.

For 84 km downwind, the predicted NO concentrations ranged from negligible during the night to 16

ppb during the day. NO₂ concentrations ranged from very small values at night to 42 ppb during daylight hours, and O₃ concentrations varied from 40 to 84 ppb. These upper range values for NO, NO₂ and O₃ exceed all of the observed background values, suggesting that 84 km downwind for this model was an

insufficient distance to be considered background. However, the lower range values for NO and NO_x, even at 84 km, were much smaller than the reported background data given above. These very low NO_x concentrations are similar to values reported by Cox (1977) for an unpolluted maritime site in Southwest Ireland. Background levels for NO were given as less

than 0.2 ppb, and the NO₂ level was 0.4 ppb. Other more recent measurements for NO₂ in relatively clean continental air indicated concentrations as low as 0.1–0.3 ppb (Noxon *et al.*, 1980) although invasion of aged polluted air masses showed concentrations of 10 ppb and even higher (Kelly *et al.* 1979). In very clean air far from major sources, NO_x concentrations can

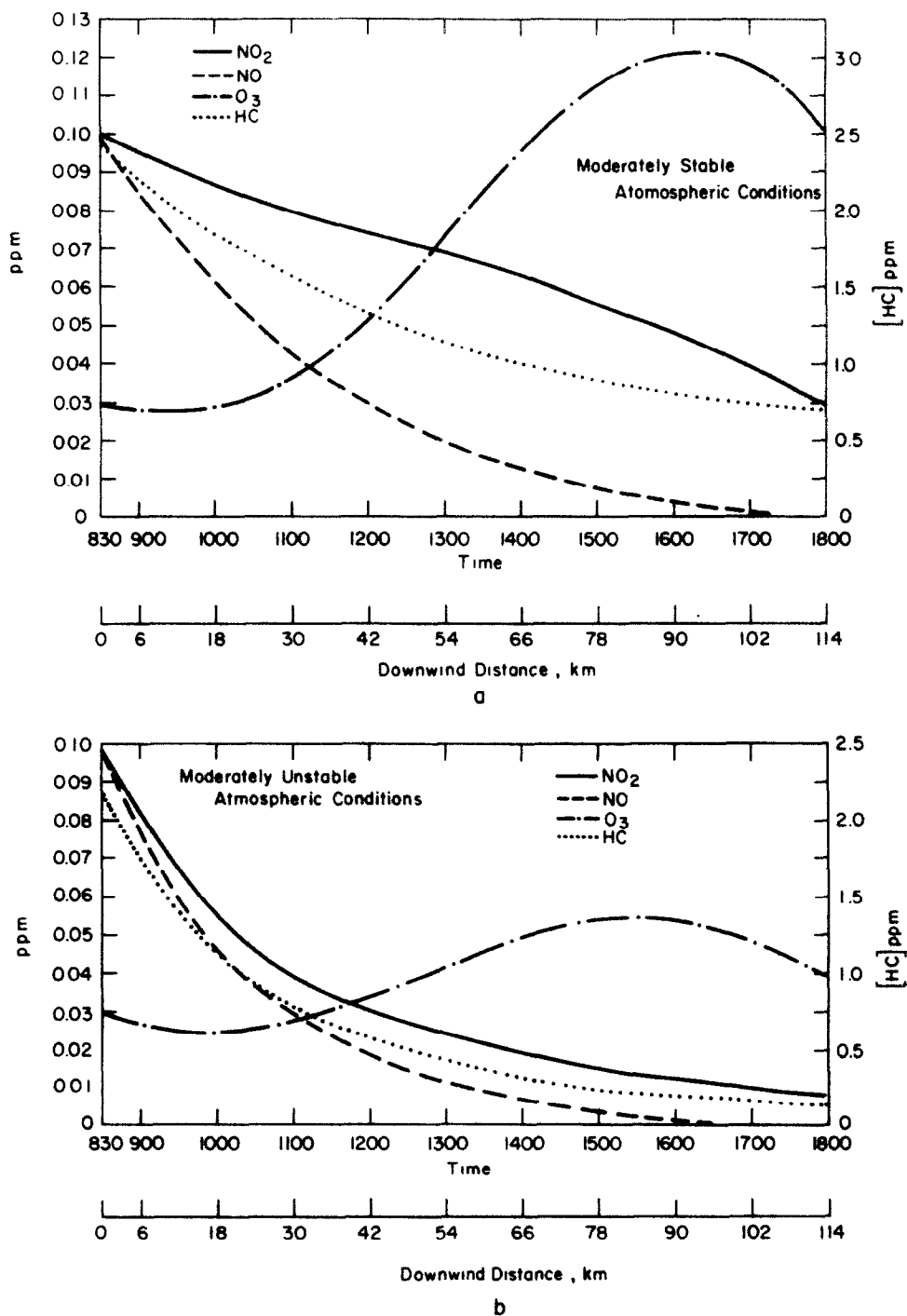


Fig. 7. Effect of atmospheric stability on the NO_x, NO₂, HC and O₃ concentrations as a function of distance or travel time from the urban area: (a) moderately stable atmospheric conditions and (b) moderately unstable atmospheric conditions.

apparently be 0.1 ppb and lower (cf. Noxon, 1975, McFarland *et al.*, 1979). These values for maritime atmospheres, and thus the lower range values of this study, would be expected to be more representative of actual background concentrations since significant sources of NO_x are not present over the ocean.

4.4. Effects of atmospheric stability

The effects of atmospheric stability are illustrated in Fig. 7. Two different Gifford-Pasquill stability categories were selected to compare to the original neutral stability simulation shown in Fig. 3(a). Figures 3(a) and 7 are for simulations for a plume emergence time of 8:30 am at neutral, moderately stable, and moderately unstable atmospheric conditions.

Figure 7(a) shows the concentration profiles for NO_2 , NO , O_3 and hydrocarbons under moderately stable atmospheric conditions. It is seen that for a more stable atmosphere, the dilution effects were relatively small resulting in higher concentrations for NO , NO_2 , O_3 and hydrocarbons than for the neutral atmosphere depicted in Fig. 3(a). For a less stable atmosphere [see Fig. 7(b)], the dilution effects were increased which led to lower concentrations. Although the concentration profiles showed substantial differences under the different atmospheric stability conditions, the fractions of NO_x and hydrocarbons remaining in the plume were not significantly affected. This was in part due to the OH concentration being affected differently than the O_3 when the dilution was varied. When the O_3 concentration was increased the OH decreased. Thus, the changes in the reaction rates of hydrocarbons and NO_x with OH and O_3 tended to offset one another.

4.5. Effects of HC/NO_x ratio

Simulations were made for a plume leaving at 8:30 am to study the effects of the initial HC/NO_x ratio on the predicted results (see Fig. 8). For the case where the initial NO_x concentration is large compared to the initial reactive hydrocarbon concentration (HC/NO_x ratio = $7.2 \mu\text{g} \mu\text{g}^{-1}$), the reactive hydrocarbon was expended before all of the NO was converted to NO_2 . Significant O_3 was not formed since an appreciable amount of NO remained after the hydrocarbons had been depleted and consumed the O_3 .

The question of what would happen when a "spent" air mass is irradiated further (i.e. under conditions where only saturated hydrocarbons remain and are being transported downwind with low NO_x levels—a high HC/NO_x ratio) was raised by Kopczynski *et al.* (1975). This situation was simulated and is also shown in Fig. 8. For these conditions (HC/NO_x = $28.8 \mu\text{g} \mu\text{g}^{-1}$), NO was rapidly converted to NO_2 with little consumption of the hydrocarbons, and O_3 accumulated as the NO concentration decreased.

Spicer *et al.* (1979) reported that very high (> 0.2 ppm) O_3 concentrations in plumes downwind of large northeastern cities can be attributed primarily to the character of the urban emissions. The present modeling study has shown similar results and indicates

that O_3 levels downwind of cities such as Houston or Birmingham ($\text{HC}/\text{NO}_x \sim 13-18 \mu\text{g} \mu\text{g}^{-1}$) might not be as high.

4.6. Downwind diurnal variation of NO_x

A simulation beginning at 11:00 am and continuing for 26 h was made to estimate the NO_x tied up during nighttime in species that, through photolysis reactions, could reproduce significant NO_x levels on the second day. Species capable of this are HONO and RONO via the reactions $\text{HONO} + \text{hv} \rightarrow \text{OH} + \text{NO}$, and $\text{RONO} + \text{hv} \rightarrow \text{RO} + \text{NO}$. The effects of the HC/NO_x ratio on this behavior were also examined.

The diurnal curve for the fraction of NO_x remaining in the plume (see Fig. 9) is reminiscent of variations observed in many urban atmospheres (Ripperton *et al.*, 1970). The fraction of NO_x remaining decreased during the day dropping to very small values after sunset. However, with sunrise and the occurrence of photolytic reactions, the fraction of NO_x increased to form a very small secondary peak.

It can be seen in Fig. 9 that the smallest HC/NO_x ratio led to higher early morning NO_x levels, apparently due to the formation of lower free radical concentrations. However, the doubled HC/NO_x ratio allowed a higher secondary NO_x peak to ultimately form. This could be due to larger levels of NO_x being stored as species capable of NO and NO_2 formation by photolytic reactions at the higher HC/NO_x ratio. Even though secondary peaks formed at very long downwind distances, their magnitudes were quite small suggesting that very little NO_x , regardless of the HC/NO_x ratio, was stored overnight as chemical species capable of forming additional NO and NO_2 by photolytic reactions on the second day.

4.7. The rate of NO_x reaction in transported urban plumes

Spicer (1980) reported NO_x transformation rates in transported urban plumes. To study NO_x reactions in an urban plume, it is important that the plume is isolated and that subsequent emissions into the plume are negligible after the air mass leaves the city. Therefore, the studies by Spicer were performed in plumes transported over the desert (Phoenix, Arizona) and over the ocean (Boston, Massachusetts). Specific air parcels, e.g. the 8:00 am air mass, were sampled just downwind of the city at mid-morning and then periodically throughout the day.

Spicer reported NO_x transformation/removal rates for transported Boston plumes in the range of $0.14-0.24 \text{ h}^{-1}$. The results were plotted in the integrated form of a first order rate equation, $\ln([\text{NO}_x]_e/[\text{NO}_x]_t)$ vs. time. $[\text{NO}_x]_e$ is the expected NO_x concentration calculated from measured initial NO_x and tracer species data if no consumption is occurring, and $[\text{NO}_x]_t$ is the concentration of NO_x actually measured at time t . The slope of the straight line represents the pseudo-first-order rate constant for the removal of NO_x from the plume.

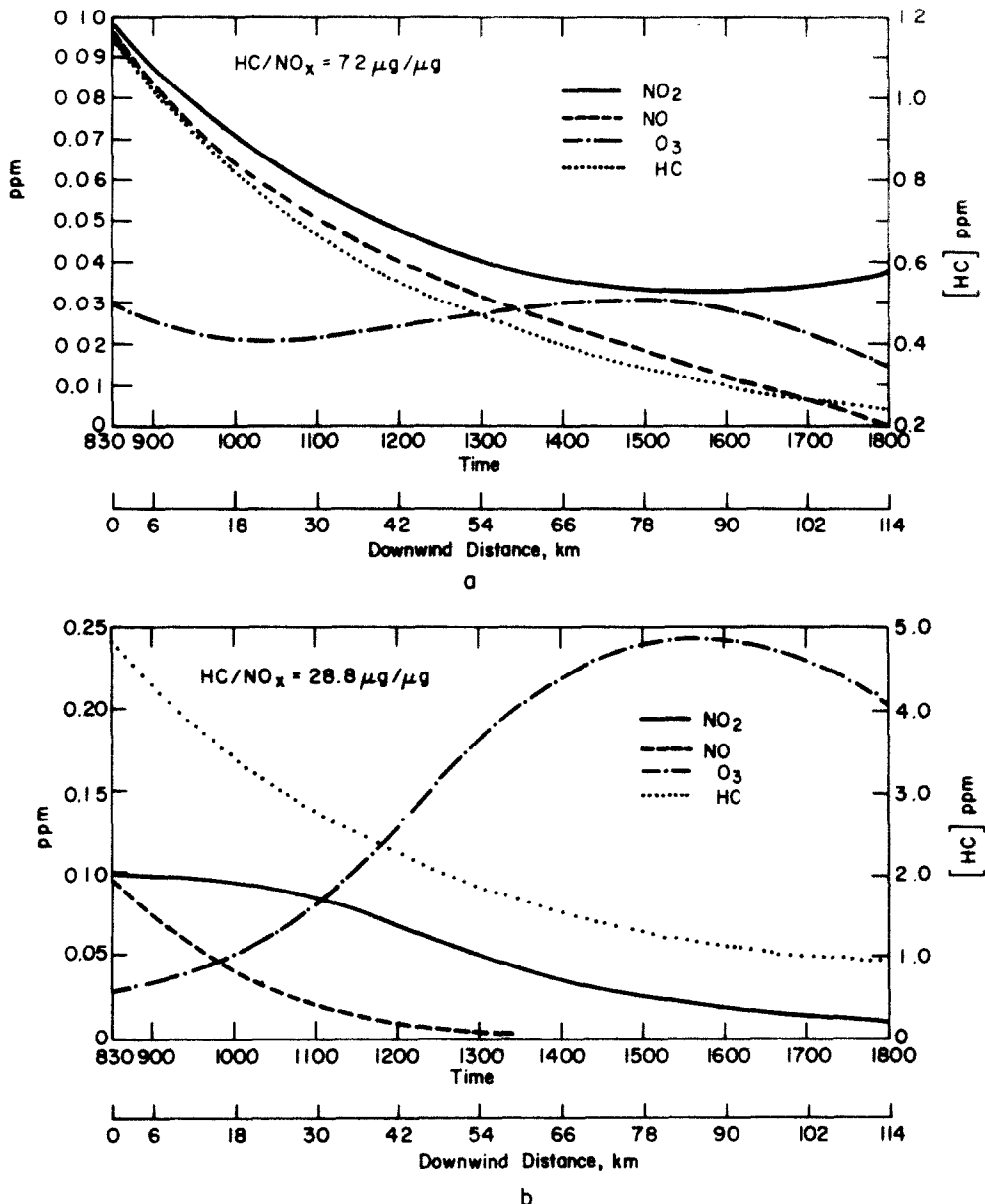


Fig. 8. Effect of HC/NO_x ratio on the NO , NO_2 , HC and O_3 concentrations as a function of distance or travel time from the urban area: (a) HC/NO_x ratio is $7.2 \mu\text{g}/\mu\text{g}$ and (b) HC/NO_x ratio is $28.8 \mu\text{g}/\mu\text{g}$.

Spicer reported that during the early stages of NO_x transformation, NO is converted to NO_2 with little net loss of NO_x . Since such behavior can cause curvature in the first order plot, the initial plume traverse was always 1–2 h after the parcel left the urban area. For this reason, the simulated data of an 8:30 am plume were plotted in a manner like the Spicer (1980) data with the 10:30 am prediction being used as the initial value. The pseudo-first-order rate constant for the simulated results with a high initial HC/NO_x ratio ($28.8 \mu\text{g}/\mu\text{g}^{-1}$), most representative of industrialized north-eastern cities, was calculated to be 0.18 h^{-1} , which is in the range reported for Boston. The first

order behavior of this study is shown in Fig. 10. It can be seen that first order kinetics do not precisely describe the Boston data.

Spicer (1980) reported NO_x transformation/removal rates for Phoenix of less than 0.05 h^{-1} . Simulated results with a lower HC/NO_x ratio ($14.4 \mu\text{g}/\mu\text{g}^{-1}$) were used to calculate a pseudo-first-order rate constant for NO_x transformation/removal which might be representative of such United States cities. The rate constant was 0.046 h^{-1} , and this simulation is also shown in Fig. 10. Spicer suggested that the low rate in Phoenix was at least partly attributable to thermal decomposition of PAN and its

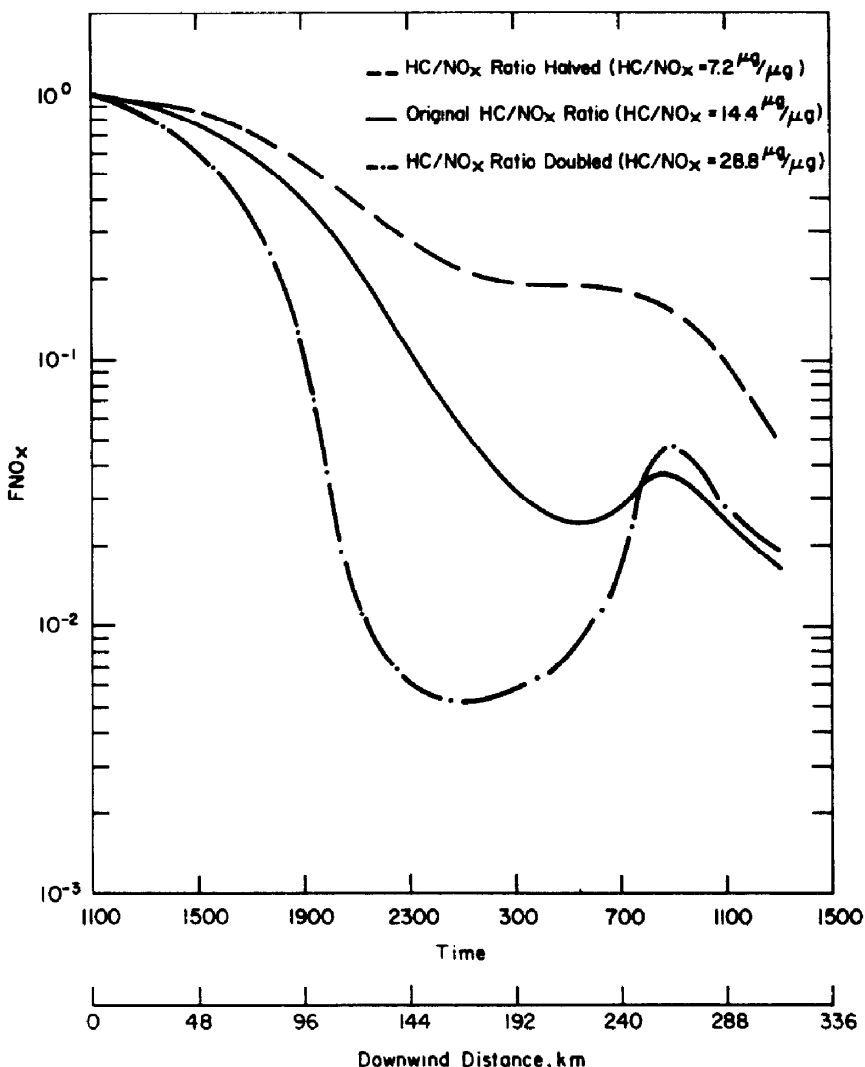


Fig. 9. Fraction of NO_x remaining in the urban plume vs. distance or travel time from the urban area for a plume emergence time of 11:00 am. This shows the small peak of NO_x formation on the second day.

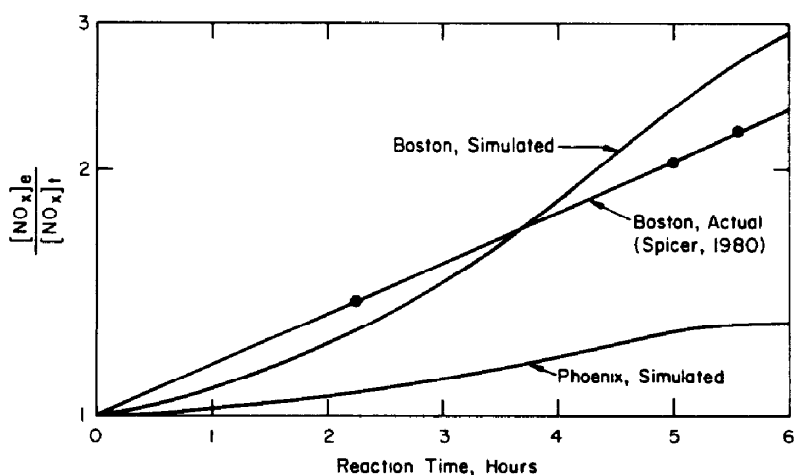


Fig. 10. Comparison of the simulation results with the data of Spicer (1980) for the Boston and Phoenix urban plumes.

analogs at the high ambient temperatures of the desert. However, this study indicates that the low rate in Phoenix was largely due to a HC/NO_x ratio lower than that characteristic of Boston.

5. CONCLUSIONS

The phenomena occurring as photochemical pollutants are emitted into an urban atmosphere and then transported a long distance to the background were simulated by incorporating dilution effects into the photochemical mechanism proposed by Falls and Seinfeld (1978). The chemically reacting and spreading plume from an urban area was examined at various plume emergence times, initial HC/NO_x ratios, and atmospheric stability conditions. Pseudo-first-order rate constants for the decomposition/transformation of NO_x at various initial HC/NO_x ratios were also calculated.

The concentration profiles for NO, NO₂, O₃ and hydrocarbons exhibited characteristics of actual urban plume activity. The NO, NO₂ and hydrocarbon levels decreased slowly with downwind distance, while the O₃ concentration increased to significant levels (~ 0.095 ppm) before peaking late in the afternoon. Only 15–30% of the initial NO_x and 25–30% of the initial olefins remained in the plume at 10:00 pm for a plume emergence time of 11:00 am. These fractions decreased as the HC/NO_x ratio increased.

Diurnal variations were detected for NO_x, but the magnitude of the peak on the second day was quite small in comparison to the primary peak, implying that relatively little NO_x was stored overnight as species that could reproduce NO and NO₂ by photolytic processes on the following day. Atmospheric stability was found to be relatively unimportant in affecting the fractions of NO_x and hydrocarbons remaining in the plume, although the actual concentration profiles were quite different.

Pseudo-first-order rate constants for the transformation/removal of NO_x were calculated to be 0.18 h⁻¹ for a high HC/NO_x ratio and less than 0.046 h⁻¹ for smaller HC/NO_x ratios. These values compare quite favorably to the measurements of Spicer (1980) for Boston (0.14–0.24 h⁻¹) and Phoenix (< 0.05 h⁻¹).

Acknowledgement—This research was supported by the National Aeronautics and Space Administration under Research Grant NSG-1424.

REFERENCES

- Breeding R. J., Lodge J. P. Jr., Pate J. B., Sheesley D. C. II., Klonis B., Fogle B., Anderson J. A., Englert T. R., Haagenson P. L., McBeth R. B., Morris A. L., Pogue R. and Wartburg A. F. (1973) Background trace gas concentrations in the Central United States. *J. geophys. Res.* **78**, 7057–7064.
- Calvert J. G. (1976a) Test of the theory of ozone generation in Los Angeles atmosphere. *Envir. Sci. Technol.* **10**, 248–255.
- Calvert J. G. (1976b) Hydrocarbon involvement in photochemical smog formation in Los Angeles Atmosphere *Envir. Sci. Technol.* **10**, 256–262.
- Cox R. A. (1977) Some measurements of ground level NO, NO₂ and O₃ concentrations at an unpolluted maritime site *Tellus* **29**, 356–362.
- Falls A. H., McRae G. J. and Seinfeld J. H. (1979) Sensitivity and uncertainty of reaction mechanisms for photochemical air pollution. *Int. J. chem. Kinetics* **11**, 1137–1162.
- Falls A. H. and Seinfeld J. H. (1978) Continued development of a kinetic mechanism for photochemical smog. *Envir. Sci. Technol.* **12**, 1398–1406.
- Fowler M. E. and Warton R. M. (1967) A numerical integration technique for ordinary differential equations with widely separated eigenvalues. *IBM Jl. Res. Dev.* **11**, 537–543.
- Gifford F. A. (1961) Uses of routine meteorological observations for estimating atmospheric dispersion. *Nucl. Safety* **2**, 47–51.
- Hampson R. F. and Garvin D., Eds. (1977) Reaction rate and photochemical data for atmospheric chemistry. *NBS Special Publication 513*, National Bureau of Standards, Washington, D.C.
- Kelly T. J., Stedman D. H. and Kok G. L. (1979) Measurements of H₂O₂ and HNO₃ in rural air. *Geophys. Res. Lett.* **6**, 375–378.
- Kitada T. (1979) A three-dimensional global model of CO and CH₄ in the troposphere. University of Kentucky, Department of Chemical Engineering, Lexington, Kentucky.
- Kopczynski S. L., Kuntz R. L. and Bufalini J. J. (1975) Reactivities of complex hydrocarbon mixtures. *Envir. Sci. Technol.* **9**, 648–653.
- McFarland M., Kley D., Drummond J. W., Schmeltekopf A. F. and Winkler R. H. (1979) Nitric oxide measurements in the equatorial Pacific region. *Geophys. Res. Lett.* **6**, 605–608.
- Mohnen V. A. and Hogan A. (1977) Ozone measurements in rural areas. *J. geophys. Res.* **82**, 5889–5895.
- Noxon J. F. (1975) NO₂ in the stratosphere and troposphere by ground based absorption spectroscopy. *Science* **189**, 547–549.
- Noxon J. F., Norton R. B. and Marovich E. (1980) NO₃ in the troposphere. *Geophys. Res. Lett.* **7**, 125–128.
- Pasquill F. (1962) *Atmospheric Diffusion*, pp. 366–380. Van Nostrand, London.
- Ripperton L. A., Korneich L. and Worth J. J. B. (1970) Nitrogen dioxide and nitric oxide in non-urban air. *J. Air Pollut. Control Ass.* **20**, 589–592.
- Spicer C. W. (1980) The rate of NO_x reaction in transported urban air. In *Atmospheric Pollution 1980, Proceedings of the 14th International Colloquium*, pp. 181–186. Paris, France.
- Spicer C. W., Joseph D. S., Sticksel P. R. and Ward G. F. (1979) Ozone sources and transport in the northeastern United States. *Envir. Sci. Technol.* **13**, 975–985.
- Stampfer J. F. and Anderson J. A. (1975) Locating the St. Louis urban plume at 80 and 120 km and some of its characteristics. *Atmospheric Environment* **9**, 301–313.
- Taylor W. D., Allston T. D., Moscato M. J., Fazekas G. B., Kozlowski R. and Takacs G. A. (1980) Atmospheric photodissociation lifetimes for nitromethane, methyl nitrite and methyl nitrate. *Int. J. chem. Kinetics* **12**, 231–240.
- Weaver J., Meagher J. and Heicklen J. (1976) Photo-oxidation of CH₃CHO vapor at 3130 Å. *J. Photochem.* **6**, 111–126.